NUMERICAL ANALYSIS OF THE AERODYNAMIC LIFT AND DRAG OVER SACCON UCAV

Normeelaiya Al-hussien[a], Nur Amalina Musa[a], Muhammad Ahmar Zuber[a] Shabudin Mat[b,*]

[a]Department of Mechanical Engineering, Faculty of Engineering, City University Malaysia, 46100 Petaling Jaya, Selangor, Malaysia
[b]UTM Aerolab, Universiti Teknologi Malaysia, 81310 UTM Johor Bahru, Malaysia

Article history
Received
8th May 2026
Received in revised form
4th June 2026
Accepted
4th June 2026
Published
15th June 2026

*Corresponding author
shabudin@utm.my

ABSTRACT

This study numerically investigates the effect of leading-edge sweep angle on the aerodynamic performance of a generic Stability and Control Configuration (SACCON) unmanned combat aerial vehicle (UCAV). Three configurations with leading-edge sweep angles of 45°, 53°, and 60° were modelled and simulated using computational fluid dynamics (CFD) in ANSYS Fluent. A virtual wind-tunnel domain with a freestream velocity of 50 m/s was used, and the simulations were performed using the Spalart–Allmaras turbulence model at angles of attack of 5°, 10°, 15°, and 20°. The lift coefficient, drag coefficient, lift-to-drag ratio, and surface pressure distribution were evaluated for each configuration. The results show that the leading-edge sweep angle influences both lift and drag characteristics, particularly at higher angles of attack. The 53° reference configuration produced higher lift and drag at 20°, while the 45° configuration showed better lift-to-drag performance at higher angles of attack. The findings indicate that leading-edge sweep modification affects the aerodynamic efficiency of SACCON-type UCAV configurations and should be considered carefully in early-stage aerodynamic design.

KEYWORDS

Leading-edge sweep angle; SACCON; CFD; UCAV

INTRODUCTION

With advances in fly-by-wire control systems, tailless and flying-wing configurations have received increasing attention because they offer potential aerodynamic, fuel-efficiency, noise, and stealth advantages [1–3]. The idea of integrating all components into a single, optimised wing is not new, and interest in this concept has surged in recent years. For both commercial and unmanned aircraft, research and interest in tailless designs continue to grow, as the configuration offers many advantages, including improved performance, fuel efficiency, reduced noise, and stealth characteristics [1-3].

According to Schutte et al. [4], for real aircraft, performance and endurance considerations often lead to medium-swept wings with sweep angles of 45° to 60° [4]. However, the aerodynamics of these configurations is characterised by unsteady, nonlinear behaviour dominated by complex vortical flow. Hence, an adequate understanding of aircraft aerodynamics is of utmost importance in aircraft design.

Tailless aircraft, such as flying wings, typically rely on variations in spanwise lift distribution to ensure stability in roll, pitch, and yaw. For Uninhabited Combat Air Vehicles (UCAVs), the combination of vehicle shaping and the manoeuvre envelope can often produce separation-induced leading-edge vortex flows. Tailless aircraft, especially UCAVs, not only have to survive through shaping for stealth but also through manoeuvrability. Their aerodynamic shape is also challenged by the complete suite of nonlinear aerodynamic behaviour.

In this study, a generic UCAV configuration, SACCON, with a blended wing-body configuration having a 53° leading-edge sweep, was used as a reference model. Later, the leading-edge sweep angle, ΛLE, was set to 45° and 60° to examine the

effect of ΛLE on aerodynamic lift and drag at various angles of attack. Computational fluid dynamics (CFD) simulations were performed to study the aerodynamic lift and drag of the models as a function of angle of attack. The reference model (53° leading-edge sweep) was used to validate the CFD code before running simulations for the other leading-edge sweep angles. The variation in leading-edge sweep angle, ΛLE, is one of the main contributors to the progression of complex vortical flow, which causes nonlinear aerodynamic behaviour [4]. The complexity of vortex flows on SACCON has affected the values of aerodynamic lift and drag [5].

SETUP AND METHODOLOGY

Model Set Up

The SACCON is an abbreviation for Stability and Control Configuration, which is a generic UCAV model, and its basic design was developed within the NATO STO/AVT-161 task group. The planform of SACCON is a lambda-wing type, with a leading-edge sweep angle of 53˚. The reference model layout used in this study has a wing span of b = 1.54m, a root chord of Cr = 1.06m and a wing area of S = 0.77 m2, as referred in Figure 1 by Huber et al. [6].

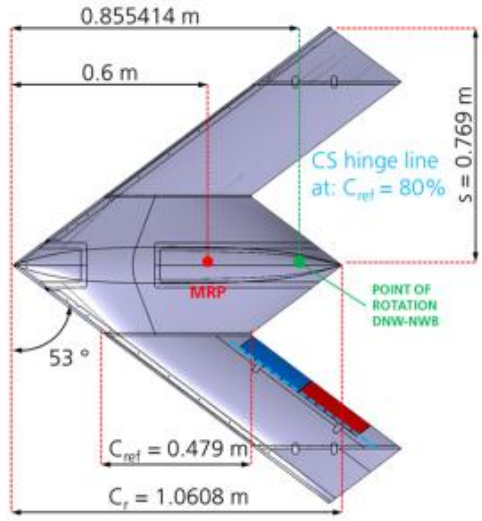

Figure 1: Model Layout of the SACCON geometric parameters adapted from [4,6]

Meanwhile, Figure 2 shows that the main sections of the model are the fuselage, the wing section and the wing tip, and its configuration is defined by three different airfoil profiles at each section, whereby the outer wing section profile has 5˚ of washout about the leading edge to reduce the aerodynamic loads and to shift the onset of flow separation to higher angles of attack [4,6]. Figure 3 and Table 1 are the 3D model and specification obtained from the NATO Research and Technology Organisation Task Group. [8, 9, 10, 11].

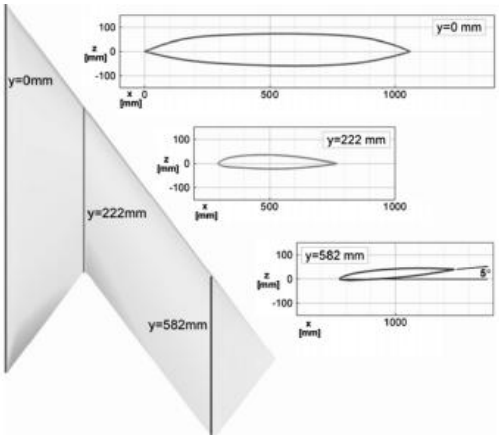

Figure 2: Planform and wing airfoil section profiles along the span of the SACCON adapted from [4,7]

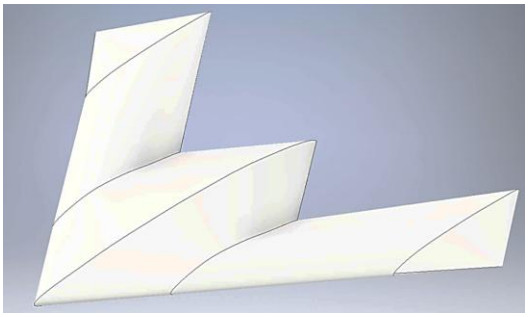

Figure 3: 3D model of SACCON with 53°

Table 1: Dimension of SACCON

Parameter	Value
Span length, b	1538 mm
Semi span, s	769 mm
Root chord, C_r	1068 mm
Reference chord, C_{ref}	479.2 mm
Tip chord, C_t	477.3 mm
Leading edge sweep angle, Λ_{LE}	53°

Despite performance and endurance considerations, medium swept wings (45°– 60°) were used, reported for UCAV-RCS, mostly used sweep in between 50° – 60°, resulting in pure deltas, diamond and lambda shaped wings. This is due to reducing large front and side projections and removing the fuselage-wing intersection, which is prone to becoming a strong RCS corner reflector [4]. A modification of the generic SACCON model using different leading-edge sweep angles, Λ_{LE} into

45°and 60° was used in this study, as shown in Figure 4, and the platform view is shown in Table 3. Meanwhile, other dimensions were maintained as in Table 1. Referring to Figure 5, the span length was maintained constant during leading-edge sweep angle modification, which resulted in the width of the chord tip changing as in Table 2.

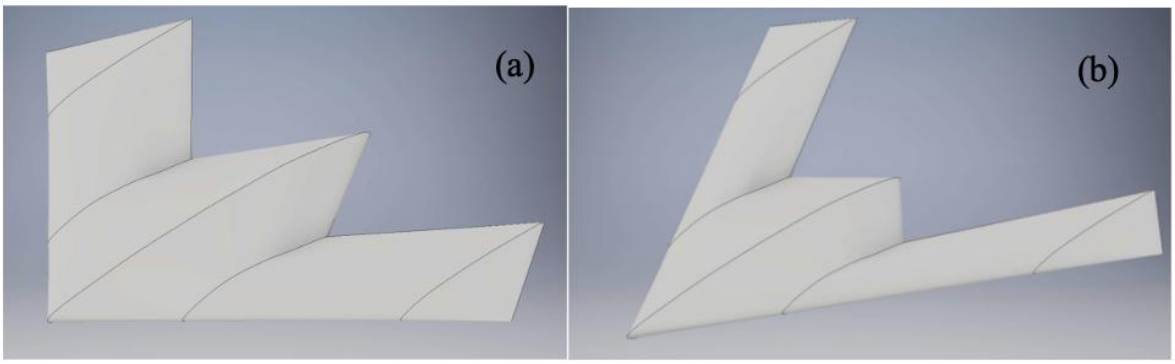

Figure 4: a) Model 2 Λ_{LE} = 45 ˚, (b) Model 4 Λ_{LE} = 60 ˚

Table 2: New Dimension of Chord Tip as a Resulted of Leading-edge Sweep Angle Modification

Parameters	References Model (Model 1)	Model 2	Model 3
Leading-edge sweep angle, ΛLE	53 ˚	45˚	60˚
Chord Tip Width (mm)	312.75	350.46	242.98

Table 3: Plant form View for each Model

Leading-edge sweep angle, ΛLE	53 ˚	45˚	60˚
Planform view with wing span	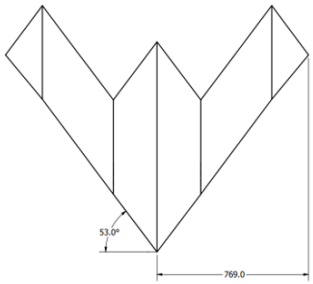	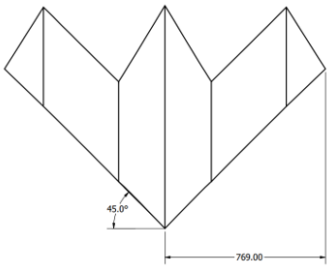	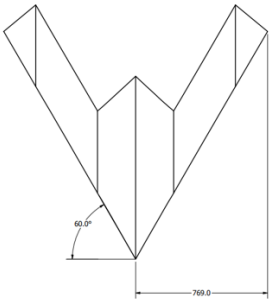
Planform view with Chord tip and surface area	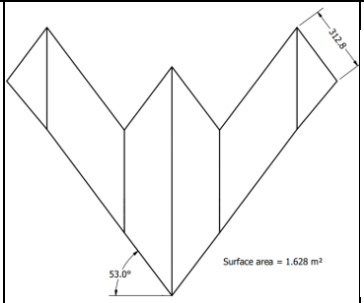	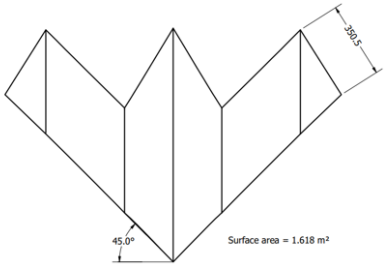	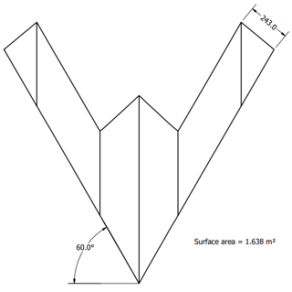

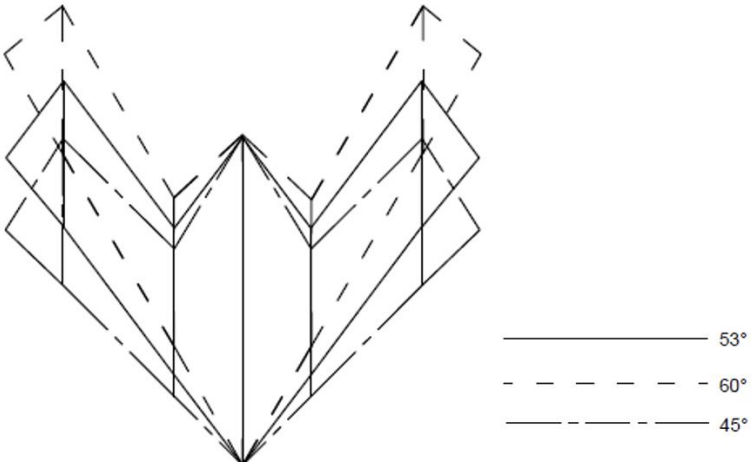

Figure 5: Effect of Leading-edge Sweep Angle Modification Affect the Aspect Ration of SACCON

The model was tested in a simulated wind tunnel using CFD to study changes in the lift and drag coefficients with different leading-edge sweep angles, with a variation in angle of attack from 5° to 20° in 5° increments. The lift and drag were measured and compared between each model. At the same time, pressure distribution was also highlighted in this study.

Simulation Set Up

The simulation for this paper was performed using ANSYS Fluent. The simulation follows the standard CFD workflow. The simulation starts with a general start-up, meshing, initial parameters and boundary conditions, turbulent model, and simulation parameters.

The first part of the simulation is to define the simulation model in the general start-up. The simulations were intended to replicate the SACCON experiment in a wind tunnel. The virtual wind tunnel is designed based on the NASA Langley 14 by 22-foot subsonic tunnel [12] and depicted in Figure 6. The SACCON model was limited to a single wing side to reduce complexity and computing time, as shown in Figure 7.

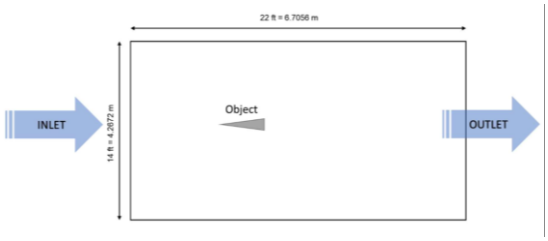

Figure 6: Virtual Wind Tunnel with Dimension

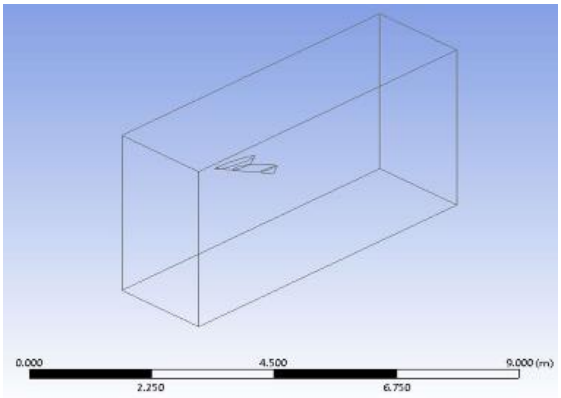

Figure 7: SACCON Isometric View Inside the Calculation Domain

The next step, the entire virtual wind tunnel and half SACCON wing inside the wind tunnel were meshed with size of 0.15 m. The mesh was generated as a tetrahedral unstructured grid to allow the solver to automatically determine the meshing parameters during meshing, which helps reduce the complexity of the computational domain. The mesh is shown in Figure 8, with a finer mesh concentrated around the SACCON model and, beyond that, automatically set by the solver.

The initial and boundary conditions are set with the inlet (the direction of the incoming wind) and the outlet (the direction of the outgoing wind), as shown in Figures 6 and 8. The wall is constrained by the wind tunnel size, and the solver is constrained to the inside of the wall. For the solver, RANS was selected, and the Spalart-Allmaras turbulent model was selected because both are widely used in the SACCON research community. Also, the Spalart-Allmaras model can be cross-referenced with other models and is

comparable to experimental results. [8,9,10,11].

The parametric values are shown in Table 4.

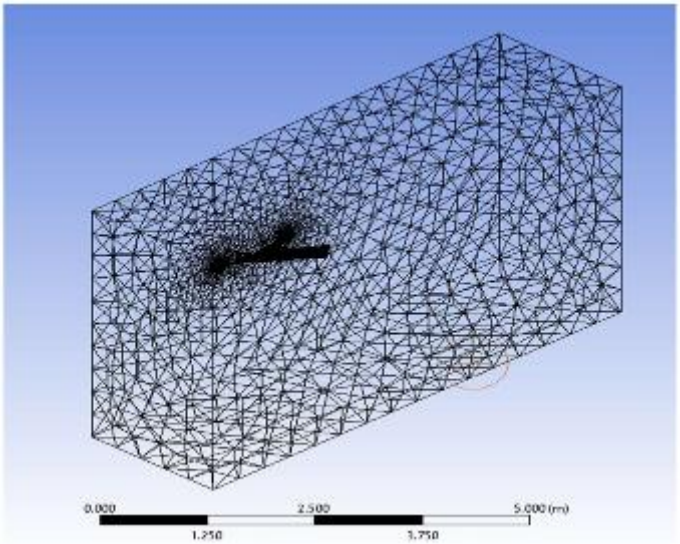

Figure 8: Meshing for the calculation domain

Table 4: Parametric value of the model and initial condition

Parameter	Value
Turbulence model	Spalart-Allmaras
Turbulent viscosity ratio	10
Inlet velocity	50 m/s
Inlet Mach number	0.146
Outlet gauge pressure	0 Pa

RESULTS AND DISCUSSION

Figures 9, 10, and 11 show the aerodynamic characteristics of the model configuration. Figures 9 and 10 show the variation in lift and drag coefficients with angle of attack. The overall lift has a similar trend for all leading edges. Only the leading-edge with 60° (model 3) configuration shows a lower lift for every AOA. This is due to the configuration being somewhere in between pure deltas, diamond and lambda-shaped wings [4]. The drag coefficient shows much greater sensitivity to changes in the leading-edge sweep angle, especially at 20° AOA for each model.

Model 1 shows a higher lift and drag coefficient at 20° AOA. Referring to Figure 11, Model 1 exhibits a better lift-to-drag ratio at lower AOA and shows an average lift-to-drag ratio between Models 2 and 3 at higher AOA. For higher AOA, Model 2 showed better efficiency than the other models. Notice that the changes in the leading-edge sweep angle affect the effectiveness of the aerodynamic characteristics of the aircraft configuration.

Table 5 shows the pressure distribution on the upper wing surface of each model as AOA varies, with the pressure increasing gradually as AOA increases. All the models show that the pressure distribution is fairly distributed at low AOA. Though the surface pressure distribution is very sensitive to small variations in AOA [4]. Later, models 1 and 2 begin to develop higher pressure at their wing tips and fuselage bodies at 15° AOA.

Meanwhile, at 20°, model 1 begins to develop a pronounced pressure distribution. This is due to the flow conditions at this angle no longer being steady, as vortex breakdown begins to establish [4]. Vallespin [13] reported that the flow around the baseline SACCON configuration, corresponding to the 53° model shown in Figure 3 and Table 1, exhibits vortex splitting caused by boundary-layer interaction. This occurs over a small range of angles of attack, approximately 10° to 15°, as the vortex onset and breakdown locations move upstream. The main source of this flow distribution behaviour is due to the variation in leading edge geometry and the wing washout [13]. However, with the leading-edge sweep angle modified to 60° (model 3), it shows a better pressure distribution across the entire AOA.

.

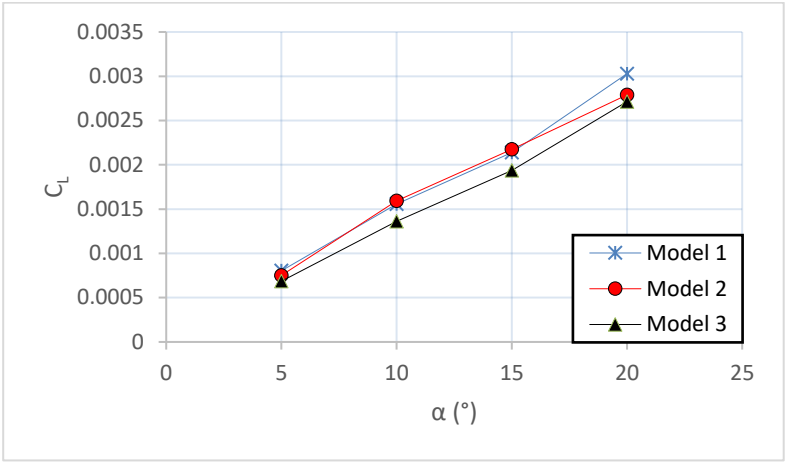

Figure 9: Lift Coefficient over AOA

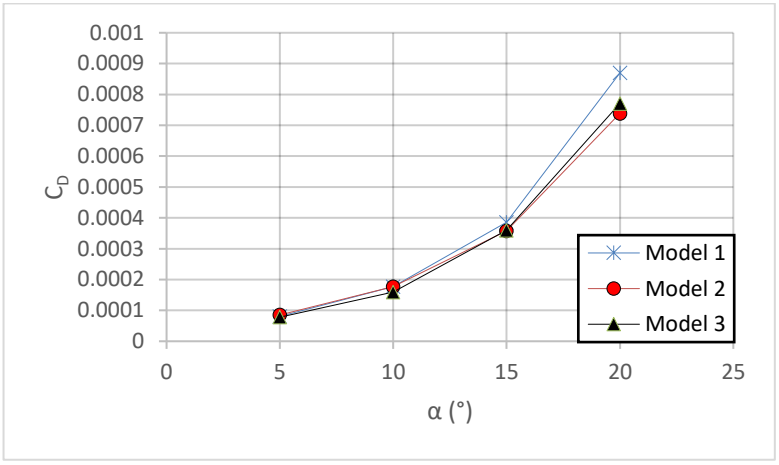

Figure 10: Drag Coefficient over AOA

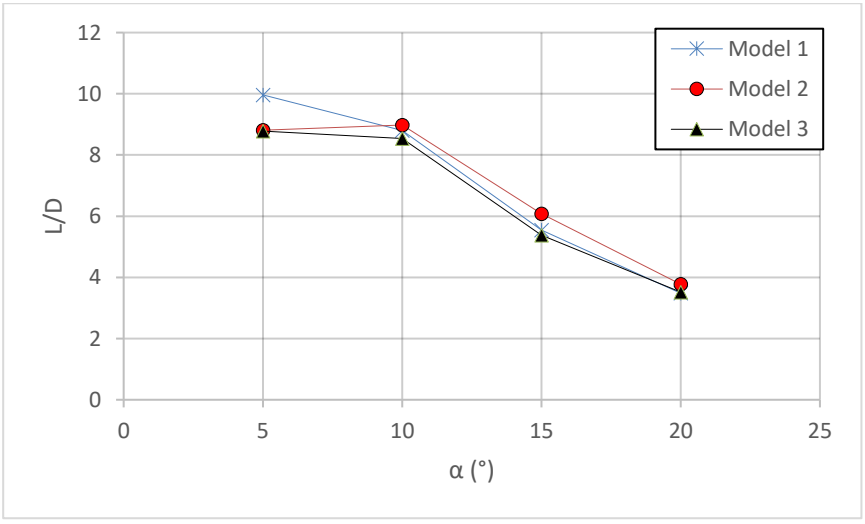

Figure 11: Lift to Drag Ratio over AOA

Table 5: Pressure Distribution Contours of the Models

AOA	Model 1	Model 2	Model 3
5˚	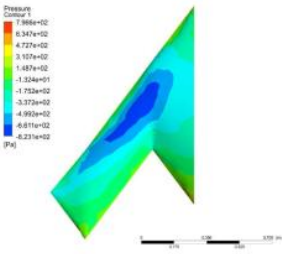	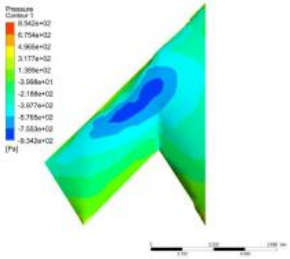	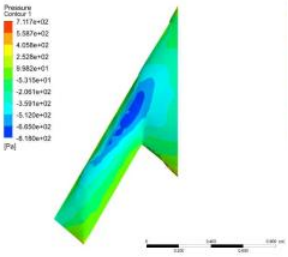
10˚	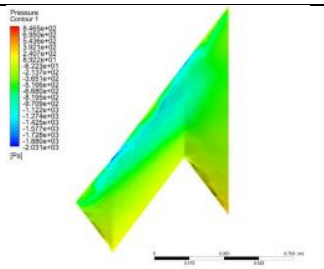	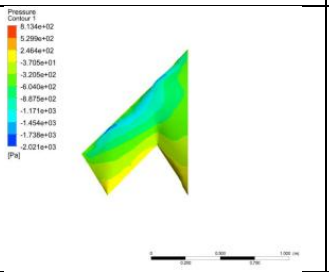	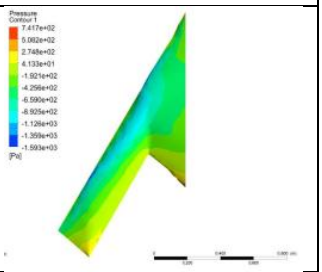
15˚	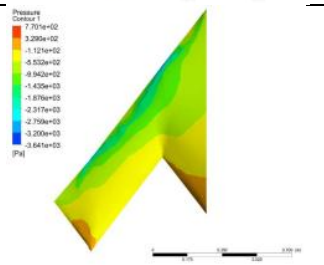	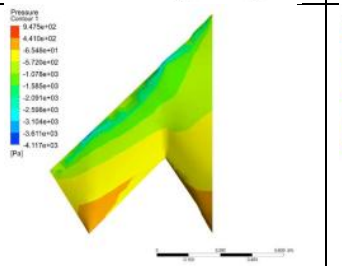	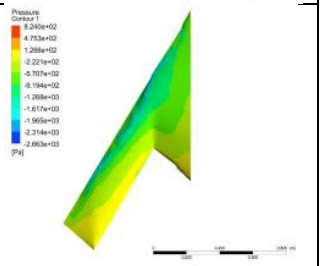
20˚	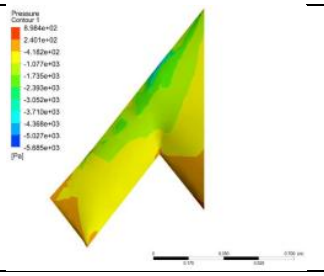	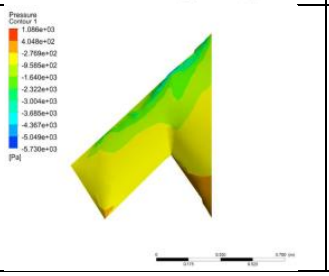	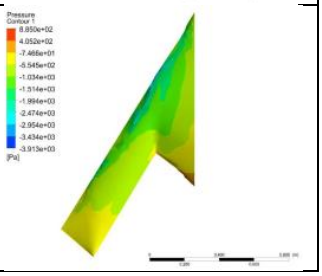

.

CONCLUSION

This study numerically examined the effect of leading-edge sweep angle on the aerodynamic performance of a SACCON-type UCAV configuration. Three sweep angles, 45°, 53°, and 60°, were evaluated using CFD simulations at angles of attack from 5° to 20°. The results indicate that leading-edge sweep angle influences the lift coefficient, drag coefficient, lift-to-drag ratio, and surface pressure distribution. The 53° baseline model produced higher lift and drag at 20°, whereas the 45° configuration showed better aerodynamic efficiency at higher angles of attack, as indicated by the lift-to-drag ratio. The 60° configuration produced lower lift across the tested angles of attack but showed a more stable pressure distribution. These findings suggest that leading-edge sweep angle is an important geometric parameter in the aerodynamic design of SACCON-type UCAVs. Future work should include grid-independence verification, quantitative validation against published wind-tunnel data, and detailed analysis of vortex structure, pressure-coefficient distribution, and flow-separation behaviour.

ACKNOWLEDGEMENT

Special acknowledgement to the technical staff of the Universiti Teknologi Malaysia Aerolab.

REFERENCES

[1] *Nickel, K., & Wohlfahrt, M. (1994). Tailless aircraft in theory and practice (E. Brown, Trans., 1st ed.). Butterworth-Heinemann; AIAA Education Series.*

[2] *Wood, R. M., & Bauer, S. X. S. (2001). Flying wings/flying fuselages. In 39th AIAA Aerospace Sciences Meeting & Exhibit (AIAA Paper 2001-0311, pp. 1–26).*

[3] *Liebeck, R. H. (2004). Design of the blended wing body subsonic transport. Journal of Aircraft, 41(1), 10–25.*

[4] *Schuette, A., Hummel, D., & Hitzel, S. (2010). Numerical and experimental analyses of the vortical flow around the SACCON configuration. In 28th AIAA Applied Aerodynamics Conference (AIAA-2010-1400).*

[5] *Luckring, J. M., et al. (2016). Objectives, approach, and scope for the AVT-183 diamond-wing investigations. Aerospace Science and Technology, 57, 2–17.*

[6] *Hübner, A.-R. (2014). UCAV model design and static experimental investigations to estimate control device effectiveness and stability and control capabilities [Doctoral dissertation]. Core.ac.uk.*

[7] *Loeser, T., Vicroy, D., & Schuette, A. (2010). SACCON static wind tunnel tests at DNW-NWB and 14 × 22 NASA LaRC. In 28th AIAA Applied Aerodynamics Conference (pp. 1–13).*

[8] *Loeser, T., Vicroy, D., & Schuette, A. (2010). SACCON static wind tunnel tests at DNW-NWB and 14 × 22 NASA LaRC. In 28th AIAA Applied Aerodynamics Conference (p. 4393).*

[9] *Schutte, A., Hummel, D., & Hitzel, S. M. (2010). Numerical and experimental analyses of the vortical flow around the SACCON configuration. In 28th AIAA Applied Aerodynamics Conference.*

[10] *Cummings, R. M., & Schutte, A. (2012). Integrated computational/experimental approach to unmanned combat air vehicle stability and control estimation. Journal of Aircraft, 49(6).*

[11] *Luckring, J. M., Boelens, O. J., Breitsamter, C., Hövelmann, A., Knoth, F., Malloy, D. J., & Deck, S. (2016). Objectives, approach, and scope for the AVT-183 diamond-wing investigations. Aerospace Science and Technology, 57, 2–17.*

[12] *Gentry, G. L., Jr., Quinto, P. F., Gatlin, G. M., & Applin, Z. T. (1990). The Langley 14- by 22-foot subsonic tunnel: Description, flow characteristics, and guide for users. NASA. NASA NTRS*

[13] *David, V. (2011). Development of a process and toolset to study UCAV flight mechanics using computational fluid dynamics (Chap. 4, pp. 50–51). University of Liverpool, United Kingdom.*